Depth Estimation from Stereoscopic Image Pairs Assuming Piecewise Continuos Surfaces

Lutz Falkenhagen
Institut für Theoretische Nachrichtentechnik und Informationsverarbeitung
Universität Hannover, Appelstr. 9A, 30167 Hannover, Germany
Email: falkenhagen@tnt.uni–hannover.de

Abstract

An algorithm for estimating reliable and accurate depth maps from stereoscopic image pairs is presented, which is based on block–matching techniques for disparity estimation. By taking neighboring disparity values into account, reliability and accuracy of the estimated disparity values are increased and the corona effect at disparity discontinuities is avoided. An interpolation of disparity values within segmented regions of homogeneous disparity enables the computation of dense depth maps by means of triangulation.

1 Introduction

Depth estimation is used in applications like 3D–modelling of natural objects [1] [2], 3D–remote handling and quality control [3]. Depth information is obtained by a triangulation of corresponding image points with known stereoscopic camera parameters. Therefore, the coordinate difference between corresponding image points, called disparity, has to be estimated. Applying common block–matching techniques for disparity estimation, the correspondence of image points is evaluated using the cross correlation or mean absolute difference of corresponding image blocks [4]. To increase the reliability of disparity estimates, large block sizes have to be chosen. On the other hand, large block sizes decrease the accuracy of disparity estimation. Hierarchical block–matching combines both, accuracy and reliability, but gives rise to corona effects at disparity discontinuities [5].

The goal of this contribution is to overcome the contradictory requirements of accuracy and reliability and to avoid the corona effect. The hierarchical block–matching will be substituted by a non–hierarchical block–matching technique, which uses small block–sizes in order to provide accuracy and to avoid the corona effect. Neighboring disparity estimates are considered in order to provide reliability. A cost function for a disparity estimator will be developed that combines block–matching with a consideration of neighboring disparity estimates.

In low textured areas and in areas which are only visible in one image, disparity cannot be estimated. These areas, called disparity gaps, have be interpolated in order to obtain dense depth maps. Therefore an interpolator has to be developed that preserves disparity discontinuities.

Chapter 2 presents the developed disparity estimation algorithm. The computation of dense depth maps from disparity is explained in Chapter 3. Depth estimation results are

presented for the image sequence 'aqua', a stereoscopic image sequence acquired by the RACE–DISTIMA project [6], and compared to common disparity estimation based on block–matching in Chapter 4 . Chapter 5 concludes this paper.

2 Disparity estimation

2.1 Model of the Stereoscopic Camera System

In the course of disparity and depth estimation, a pinhole camera model based on the central projection of diffuse illuminated and diffuse reflecting spatial points in the image plane is applied. No lense distortion is considered. Each camera is defined by its position $\vec{C}$, its optical axis $\vec{A}$ and its image plane, which is determined by two perpendicular vectors $\vec{H}$ and $\vec{V}$. The camera is therefore called CAHV–camera [7]. The projection of a spatial point $\vec{P}_S = (P_{Sx}, P_{Sy}, P_{Sz})$ into the image plane of a CAHV–camera can be computed using equation (1).

$$\vec{P} = \begin{pmatrix} P_h \\ P_v \end{pmatrix} \quad with \quad P_h = \frac{(\vec{P}_S - \vec{C}) \cdot \vec{H}}{(\vec{P}_S - \vec{C}) \cdot \vec{A}} \quad , \quad P_v = \frac{(\vec{P}_S - \vec{C}) \cdot \vec{V}}{(\vec{P}_S - \vec{C}) \cdot \vec{A}} \tag{1}$$

For DISTIMA image sequences, only the intrinsic and relative extrinsic camera parameters are known, which is sufficient for depth estimation. The absolute camera parameters needed for the CAHV–camera model can therefore be chosen arbitrarily for one of the cameras. Here, the left camera is arranged in the center of the coordinate system and the right camera is positioned with respect to the known relative camera parameters (Fig. 1). Due to the emulation of human vision in DISTIMA, both cameras are arranged horizontally with a base length *b* and their optical axes have a small convergence angle ϕ. The focal length of both cameras is identical.

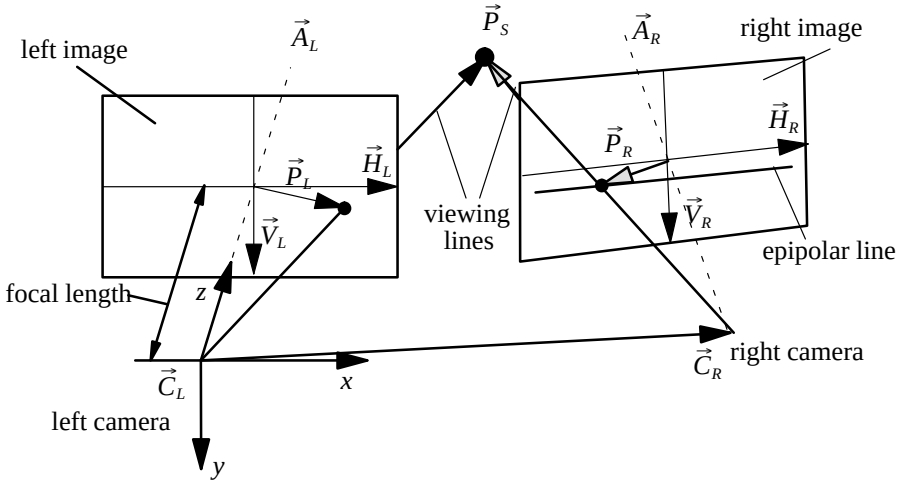

Fig. 1: Model of the stereoscopic camera system

When depth shall be estimated, the spatial position of a point has to be reconstructed from to known image coordinates of its projection in the stereoscopic image planes. The

spatial position of the point is the intersection of both viewing lines. If the viewing lines are skewed, the spatial position is assumed to be located at the point with minimal distance to both viewing lines.

The direction of the viewing lines is determined using the CAHV–camera parameters and the image coordinates. Evaluating the projection equation (1) the direction appears to be the following vector product.

$$\vec{S} = \left(\vec{A} \cdot \vec{P}_h - \vec{H}\right) \times \left(\vec{A} \cdot \vec{P}_v - \vec{V}\right) \tag{2}$$

The vector $\vec{M}$ links both viewing lines at the location of minimal distance.

$$\vec{M} = \vec{C}_R + \lambda \cdot \vec{S}_R - \vec{C}_L - \mu \cdot \vec{S}_L \tag{3}$$

Therefore $\vec{M}$ has to be perpendicular to both viewing lines $\vec{S}_L, \vec{S}_R$.

$$\vec{M} \cdot \vec{S}_L = 0 \quad , \quad \vec{M} \cdot \vec{S}_R = 0 \tag{4}$$

Based on condition (4), λ and μ are computed with equation (5).

$$\lambda = \frac{\vec{C}_L \cdot \vec{S}_L + \mu \cdot \vec{S}_L{}^2 - \vec{C}_R \cdot \vec{S}_L}{\vec{S}_L \cdot \vec{S}_R} \tag{5}$$

$$\mu = \frac{\left((\vec{C}_L - \vec{C}_{R)} \cdot \vec{S}_R\right) \cdot \left(\vec{S}_L \cdot \vec{S}_R\right) - \left((\vec{C}_L - \vec{C}_R) \cdot \vec{S}_L\right) \cdot \vec{S}_R{}^2}{\vec{S}_L{}^2 \cdot \vec{S}_R{}^2 - (\vec{S}_L \cdot \vec{S}_R)^2}$$

Finally the spatial position is determined using equation (6).

$$\vec{S}_P = 0.5 \cdot \left(\vec{C}_R + \lambda \cdot \vec{S}_R + \vec{C}_L + \mu \cdot \vec{S}_L\right) \tag{6}$$

This equation will be used for the computation of depth maps from disparity maps.

2.2 Disparity Estimation Constraints

The entity of disparity estimation is the search for corresponding image features in a stereoscopic image pair. Corresponding image features are projections of the same object feature into both image planes. Due to physical laws of image acquisition, a number of constraints for matching features can be derived. These constraints are mainly applied in feature based disparity estimation algorithms, where luminance features are extracted from the images in a first step and the disparity of these features is estimated in a second step [4].

In most area–based disparity estimation algorithms, not all of these constraints are considered, because disparity is estimated for each image point or block of image points independently. In the following, these constraints are explained.

2.2.1 Epipolar Constraint

With the applied camera model an image point $\vec{p}_L$ results from the central projection of a spatial point $\vec{P}_S$ into the left image plane. The viewing line is the connection of the spatial point $\vec{P}_S$ and the center of the camera $\vec{C}$. The projection of the viewing line into the other image plane results in the epipolar line (Fig 1). Therefore the corresponding

point in the right image plane $\vec{p}_R$ has to lie on the epipolar line, which reduces the search area of the disparity estimation to one dimension.

Under the assumption of a small convergence angle between both optical axes and a horizontal arrangement of the cameras, the epipolar line is approximately horizontal.

2.2.2 Extended Continuity Constraint

Under the assumption of large objects with a smooth surface shown in the stereoscopic image pair, the disparity varies continuously in most parts of the image. Disparity discontinuities are allowed at object boundaries only. Therefore, disparity discontinuities have to be detected and involved in the disparity estimation algorithm.

2.2.3 Disparity Gradient Limit

The possible disparity gradient is limited, because disparity changes coincide with depth changes and therefore with an occlusions of object parts in one of the images in case of high gradients. Assuming horizontally arranged cameras, for the left disparity map an upper disparity gradient of size +1 and for the right disparity map a lower disparity gradient of –1 results. The disparity gradient limits are given in equation (7).

$$\begin{aligned} -\infty < \frac{\partial d_h}{\partial h} \leq +1 \quad & \text{for the left disparity map} \\ -1 < \frac{\partial d_h}{\partial h} \leq +\infty \quad & \text{for the right disparity map} \end{aligned} \tag{7}$$

2.2.4 Monotonic Ordering Constraint

With a defined order of points along a line in one image of the image pair, the corresponding points have to occur in the same order in the other image. This constraint will be of interest when the scan line oriented disparity estimation algorithm is introduced.

2.2.5 Luminance constraint

Correspondence analysis is disturbed by camera noise. For a reliable disparity estimation, the local luminance variance σ^2_{Ih} within the compared image blocks in direction of the epipolar line has to be clearly higher than the camera noise variance σ^2_n. Therefore correspondence analysis is restricted to points $\vec{P}$ with high local luminance variance σ^2_{Ih}.

$$\sigma^2_{Ih} = \frac{1}{b}\sum_{i=-b2}^{b2}\left[\frac{1}{b}\sum_{j=-b2}^{b2} I^2(P_h\text{–}j; P_v\text{–}i) - \left(\frac{1}{b}\sum_{j=-b2}^{b2} I(P_h\text{–}j; P_v\text{–}i)\right)^2\right] \gg \sigma^2_n \tag{8}$$

with b = blocksize and b2 = (blocksize–1) / 2

2.3 Disparity Estimation considering Directly Neighboring Disparity Values (DN–Cost Function)

In order to estimate a dense disparity map for an image, for each point of the image a corresponding point is searched in the other image. This pair of points is denoted as candidate pair. In common area–based algorithms, each possible corresponding point,

denoted as candidate, is evaluated using the luminance difference or the cross correlation of surrounding image blocks. For reliable estimation, large block sizes from 11x11 pel to 17x17 pel are needed for block–matching or in the first level of hierarchical block–matching. These block sizes giving rise to corona effects at disparity discontinuities, e.g. at object boundaries [5] and leading to less accurate disparity estimates, if no further estimation with smaller block sizes is applied.

Some of the estimation constraints mentioned in Chapter 2.2 cannot be taken into account, when disparity is estimated for each point independently. Therefore a simultaneous disparity estimation for all points along one scan line has been proposed [8]. There, a maximum likelihood cost function is employed, evaluating the luminance difference of the candidate pair and the disparity change along the scan line. This cost function is minimized for each scan line using a dynamic programming strategy. With this method all mentioned estimation constraint expect the extended continuity constraint are considered.

The first of the two presented cost functions is based on [8], but evaluating the Normalized Cross Correlation NCC (9) of a candidate pair instead of the luminance difference.

$$NCC(\vec{P}_L;\vec{P}_R) = \frac{\sum_{i=-b2}^{b2}\sum_{j=-b2}^{b2}\left(I_L(P_{Lh}-i;P_{Lv}-j)-\bar{I}_L\right)\cdot\left(I_R(P_{Rh}-i;P_{Rv}-j)-\bar{I}_R\right)}{\sqrt{\sum_{i=-b2}^{b2}\sum_{j=-b2}^{b2}\left(I_L(P_{Lh}-i;P_{Lv}-j)-\bar{I}_L\right)^2\cdot\sum_{i=-b2}^{b2}\sum_{j=-b2}^{b2}\left(I_R(P_{Rh}-i;P_{Rv}-j)-\bar{I}_R\right)^2}}$$

with $\bar{I}$ = mean luminance of a block (9)

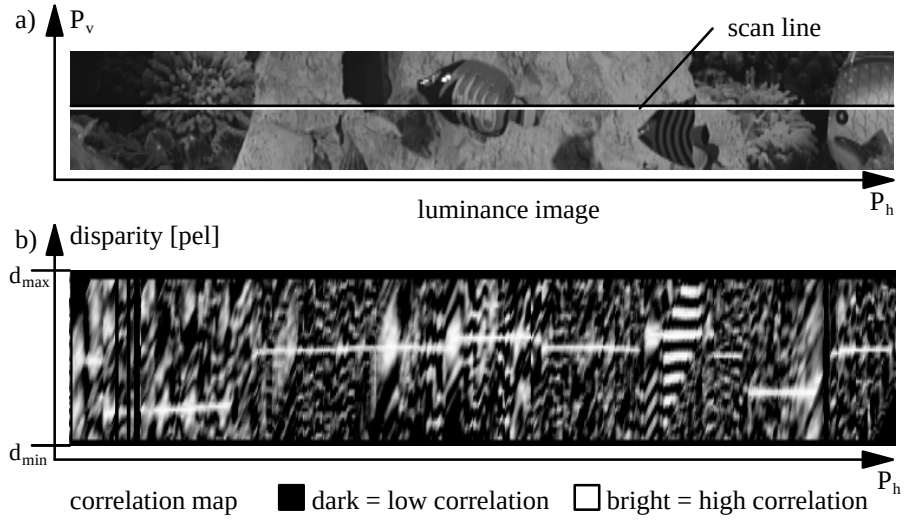

Fig. 2: a) Horizontal slice of an image from the DISTIMA test sequence 'aqua' with a selected scan line
b) Correlation map of the selected scan line, showing the NCC between each point along the scan line and each candidate on the epipolar line

In order to estimate the disparity for a scan line, a NCC map is computed, specifying the NCC for each possible candidate pair. Possible candidates are image points within a fixed disparity range. A cross correlation map for two scan lines of the test image pair 'aqua' is shown in Fig. 2, where bright horizontal lines indicate probable areas of continuos disparity. Based on the correlation map a cost map is computed applying a cost function for each candidate pair.

2.3.1 Evaluation of the DN–Cost Function

A dynamic programming strategy is applied to find the maximum likely disparity estimates for each scan line. With this strategy the cost of the candidate pairs are computed one after another starting with $h_j = 1$ and $d = d_{max}$. The cost for each candidate pair is composed of two summands, a local cost and the cost of the most probable predecessor.

For each candidate pair three possible predecessors are evaluated using (10), which have a maximum disparity difference of $\Delta d = \pm 1$ (see Fig. 3). Depending on the disparity difference the local cost is a fixed cost C_{change} for changed disparity or a matching cost C_{match} for constant disparity. The predecessor that leads to the minimal resulting cost is chosen and its position is stored additionally, in order to find the most likely way for the whole scan line.

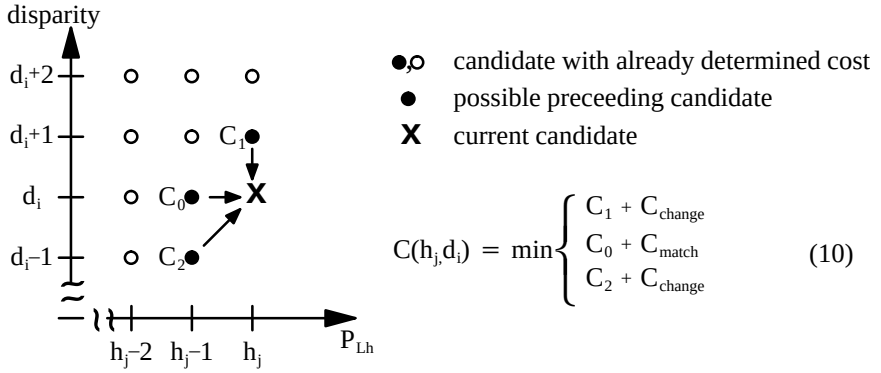

Fig. 3: Computation of the cost map with the DN–cost function

When the complete cost map of a scan line is computed, the disparity candidate with the lowest cost is searched at the last pel of the scan line. Starting from this candidate the disparity values along the scan line are determined backwards, using the path that is stored for each cost element pointing to the predecessor.

2.3.2 Elements of the DN–Cost Function

The cost for a change in disparity C_{change} depends on the probability of an object boundary $P_{boundary}$ and on the image noise variance σ_n^2. $P_{boundary}$ depends on size of the objects in the scene and is determined by the mean number of object boundaries along a scan line of the image related to the number of pels in each scan line. $P_{boundary}$ is of size 0.95 –0.98. In [8] the following cost value is derived.

$$C_{change} = \ln\left(\frac{1 - P_{boundary}}{P_{boundary}} \cdot \frac{1}{\sqrt{2\pi\sigma_n^2}}\right) \tag{11}$$

On the other hand a matching cost C_{match} has to be derived, evaluating constant disparity along the scan line. This cost value depends on the NCC of the candidate pair and has to be adapted to the size of C_{change}, which is related to the noise variance of the luminance signal. Therefore the NCC is scaled in the range of the luminance values.

$$C_{match} = 255 \cdot \frac{1 - NCC^2}{4 \cdot \sigma_n^2} \tag{12}$$

2.4 Disparity Estimation considering an Extended Neighborhood (EN–Cost Function)

The DN–cost function derived in Chapter 2.3 does not consider all estimation constraints. An extended maximum likelihood cost function is presented in this Chapter that considers additionally the extended continuity constraint. This constraint requires the examination of more than three preceding candidates. The examination is still limited to candidates in the same scan line and the new maximum likelihood cost function is minimized for each scan line using dynamic programming.

The EN–cost function is composed of three cost terms. The first cost term is the cost of the predecessor. The second cost is the cost for matching probability of a candidate pair. This cost term is similar to the one in the previous cost function, but is considered independently on the disparity change. In the previous cost function, this term was considered only in the case of constant disparity.

The third cost term $C_{penalty}$ evaluates the disparity change with respect to the predecessor. Due to the resolution of disparity, changes are limited to integer values. The evaluation of disparity changes in the left disparity map is listed below.

- Case 1: $\Delta d = 0 \Rightarrow C_{penalty} = 0$
  Continuous disparity due to an object surface parallel to the image plane.
- Case 2: $\Delta d = \pm 1 \Rightarrow C_{penalty} = C_{inclination}$
  Continuous disparity change due to the inclination of an object surface with increasing or decreasing distance to the camera
- Case 3: $-\infty < \Delta d < -1 \Rightarrow C_{penalty} = C_{discontinuity}$
  Disparity discontinuity due to a transition from an object in the foreground to an object in the background.
- Case 4: $+1 < \Delta d < +\infty \Rightarrow C_{penalty} = C_{discontinuity} + \Delta d \cdot C_{occlusion}$
  with $\Delta d = d(h_0) - d(h_0 - \Delta d)$
  Disparity discontinuity due to a transition from an object in the background to an object in the foreground, considering possible occlusions.

Because of the asymmetric disparity gradient limit, two different kinds of disparity discontinuities have to be considered. These discontinuities are denoted as Case 3 and Case 4 in the list above. For rising disparity, a discontinuity coincides with an occluded

area in the right image. As a result, disparity is undetermined in the left image within a range of Δd preceding image points. In the cost function this is considered by taking $C(h_0\text{–}\Delta d, d_0\text{+}\Delta d)$ as a possible predecessor. An additional penalty is required, evaluating the number of skipped disparity estimates. For falling disparity, a discontinuity does not coincide with an occlusion.

The cost map is determined in a similar manner as in the previous algorithm. In contrast to the previous cost function, where three predecessors have been evaluated for each candidate, the number of possible predecessors is now predestinated by the disparity range.

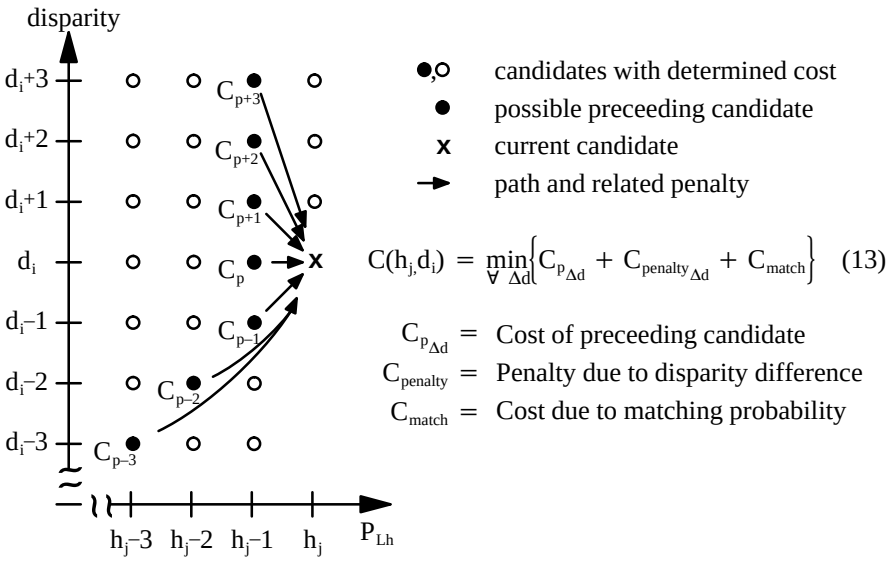

Fig. 4: Computation of the cost map with the EN–cost function

The computation of the cost of a single candidate pair is illustrated in (Fig. 4). In this Figure, each point is one element of the cost map. From each predecessor an arrow points to the current candidate, which coincides with a penalty depending on the change of disparity. The reason for the asymmetric arrangement of possible candidates is the asymmetric disparity gradient limit.

The quality of disparity estimation depends to great extent on the penalty terms of the EN–cost function (13). These penalty terms have been optimized with respect to the penalty term of the DN–cost function C_{change} using the DISTIMA test sequences.

$$\begin{aligned} C_{inclination} &= C_{change} \\ C_{discontinuity} &= 4 \cdot C_{change} \\ C_{occlusion} &= 4 \cdot C_{change} \end{aligned} \qquad (14)$$

3 Computation of a Dense Depth Map

Disparity cannot be estimated in low textured areas and in areas which are visible in one image only. These disparity gaps shall be interpolated without a smoothing of disparity discontinuities. Additionally the corona effect of block–matching shall be compensated.

3.1 Segmentation of Regions of Homogeneous Disparity

With the applied disparity estimation algorithm, disparity is estimated in pel resolution. Because of the disparity gradient limit introduced in Chapter 2.2.3 and the disparity resolution, all disparity estimates with an absolute disparity difference to their neighbors below 2 pel shall be merged into one region of homogeneous disparity. The resulting regions are therefore not limited to a certain amount of different disparity values, but to a maximum absolute disparity gradient of 1.

The segmentation is carried out in several steps. Initially, all neighboring points with equal disparity are merged into regions of constant disparity. In a second step neighboring regions with a maximum disparity difference of one are merged. In order to compensate single disparity estimation failures, a minimum connection of 10 pel between these regions is additionally required. In a third step small labels are assigned to the neighbor with the most similar disparity, which guarantees a minimum size of regions. Undetermined regions are treated as occlusions and are therefore ascribed to the deepest neighbor, which is the one with the lowest disparity.

Even with the small block–sizes of the developed disparity estimation algorithms, the corona effect of block–matching is apparent in the disparity maps (Fig. 5b). Under the assumption that object boundaries and therefore disparity discontinuities coincide with luminance edges, the corona effect of block–matching is compensated by adapting region boundaries to neighboring luminance edges. The maximum size of the corona is half of the block–size. Therefore luminance edges in this area around region boundaries are detected by evaluating the luminance gradient. Both, luminance edges and region boundaries are then dilated and afterwards skeletonized, resulting in a new region boundary in the middle between their original position. When this method is applied iteratively, the region boundaries are successively adapted to neighboring luminance edges (Fig. 5d).

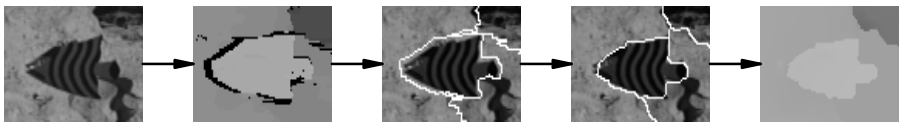

a) b) c) d) e)

Fig. 5: a) Part of DISTIMA image 'aqua'
b) Estimated disparity map (dark = low disparity, bright = high disparity)
c) Segmentation into regions of homogeneous disparity
d) Adaptation of region boundaries to neighboring luminance edges
e) Interpolated disparity map with corona compensation

3.2 Disparity Interpolation

In order to compute dense depth maps, disparity gaps have to be interpolated. Disparity discontinuities are not effected, because disparity is interpolated within segmented regions of homogeneous disparity only.

For interpolation purposes, the disparity estimates of a segmented region are approximated by a thin plate. The finite element method is used to minimize the energy of the thin plate, which is connected to the disparity values with springs of different force. The force of the springs is controlled by the reliability of the estimated disparity, which is the NCC in the proposed method. Springs of no force are applied to disparity gaps. In addition springs of no force are applied to region boundaries, because disparity estimation is unreliable due to the corona effect there. The hierarchical interpolation algorithm minimizing the energy of the thin plate is based on [9].

The reliability of disparity estimation is enhanced before the interpolation, using a disparity verification between the left and right disparity map. With this verification all disparity estimates that differ more than 1 pel from their corresponding disparity estimate in the other disparity map are neglected (15).

$$\left| d_L(h_i; v_j) - d_R(h_i - d(h_i; v_j); v_j) \right| \leq 1 \tag{15}$$

This verification enables also an assessment of disparity estimation, because the remaining disparity estimates can be treated as correct disparity values.

3.3 Depth Computation from Disparity

With known extrinsic camera parameters depth is computed from disparity. Therefore each point of the interpolated disparity map is evaluated using equation (6).

4 Results

The developed algorithms have been examined using DISTIMA stereoscopic image sequences. In this paper the results for image sequence 'aqua' are presented, which are typical for the results obtained with other image sequences. Image sequence 'aqua' has TV resolution and is 2 seconds long. The first image pair and results are presented in (Fig. 6).

Disparity has been estimated for each field of 'aqua', applying block–matching, The DN–cost function and the EN–disparity estimation use block sizes of 5x5 pel. An example of the disparity estimation results is given in (Fig. 6). To compare the three different estimation algorithms, the amount of correct disparity estimates is evaluated. The correctness is verified using (15). For 25% of the image, no disparity can be estimated, because the luminance constraint is not fulfilled of the points are only visible in one of the images of an image pair. For the remaining 75% disparity can be estimated. The part of verified disparity values rises from 65% applying block–matching to 70% with the new approaches. The difference between both new approaches is below 1%. The increased number of correctly estimated disparity values shows the result from the increased reliability of the developed algorithm. Even the consideration of an extended

neighborhood increases the reliability slightly, so that the usage is only recommended if the computation time is not relevant. Applying the proposed algorithm increases the computational effort by a factor of 2 in the case of the DN–cost function and by the factor of 3 in the case of the EN–cost function when compared to block–matching.

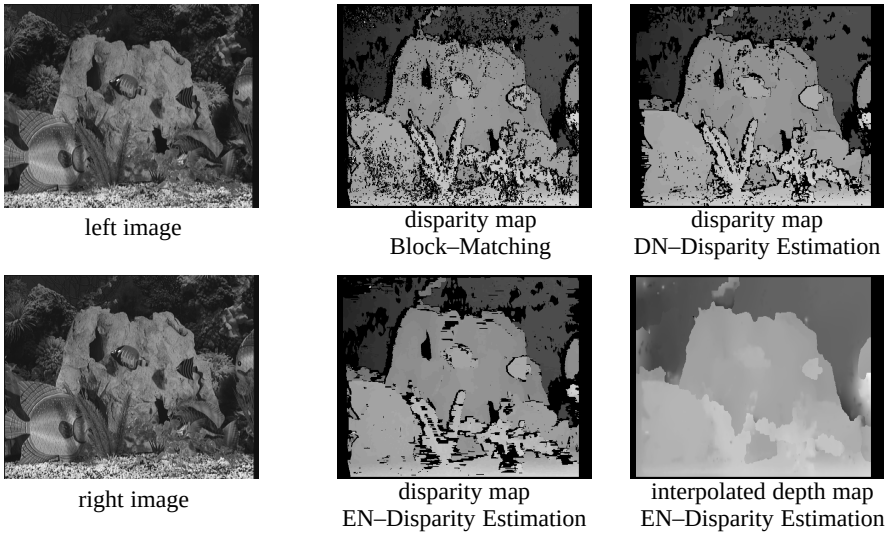

Fig. 6: Depth and disparity estimation results for a DISTIMA image pair 'aqua'

5 Conclusions

In this contribution, an algorithm for reliable and accurate disparity estimation has been developed that avoids the corona effect of block–matching at disparity discontinuities. Therefore, a disparity estimator for two corresponding lines of a stereoscopic image pair has been developed that evaluates neighboring disparity estimates. Under the assumption of horizontally arranged cameras, corresponding lines, which are also called epipolar lines, are according scan lines.

For the evaluation of neighboring disparity estimates a cost function and a cost minimization procedure has been developed that considers the following disparity estimation constraints. Each picture element (pel) of one scan line corresponds exactly to one pel of the epipolar line. Corresponding pels have to occur in the same ordering in both scan lines. These constraints are fulfilled by applying dynamic programming for the minimization of the cost function. The disparity gradient in horizontal direction is limited between $[-\infty ; +1]$, which reduces the amount of possible neighboring disparity values. With the extended disparity continuity constraint, large objects are assumed and disparity discontinuities are allowed at object boundaries only. Therefore penalty terms evaluating disparity changes between neighboring disparity values are applied that cause continuos disparity to be favoured. The correspondence measure between two pels is the cross correlation of corresponding image blocks. Two cost functions have been derived, which differ in the number of considered neighbors. The first algorithm

evaluates only direct neighboring disparity estimates (DN–cost function), which enables the consideration of all constraints except the extended continuity constraint. The second algorithm evaluates an extended neighborhood (EN–cost function), which enables the consideration of all constraints.

Block sizes between 11x11 pel and 17x17 pel are chosen for block–matching or in the first level of hierarchical block–matching, in order to give reliable results. With the new cost functions the necessary block size for reliable disparity estimates is reduced to 5x5 pel. Due to the reduced block size disparity can be estimated more accurate compared to block–matching and the corona effect at disparity discontinuities can be reduced effectively compared to hierarchical block–matching. Reliability is ensured by the consideration of neighboring disparity values. The reliability of disparity estimates is verified by comparing disparity estimates of the left disparity map with corresponding disparity estimates in the right disparity map. Disparity values that do not match are deleted in the disparity map. Disparity is only be estimated, when the local luminance variance in direction of the epipolar line is much higher than the camera noise variance. Disparity estimation result for DISTIMA image sequence 'aqua' are presented. In this sequence, approximately 75 % of all image points are visible in both images and fulfill the luminance constraint. Averaged over the 50 frames, the percentage of verified disparity values is increased from 65% using block–matching to 69% using the DN–cost function and 70% using the EN–cost function. Verifications using other DISTIMA image sequences provided similar results. Applying the proposed algorithm increases the computational effort by a factor of 2 in the case of the DN–cost function and by the factor of 3 in the case of the EN–cost function when compared to block–matching.

In order to compute dense depth maps, disparity gaps have to be interpolated without a smoothing of disparity discontinuities. Therefore the disparity map is segmented into regions of homogeneous disparity. The developed segmentation algorithm subdivides the disparity map, which is estimated with integer resolution, into regions of equal disparity values in a first step. It is assumed that disparity changes between neighboring pels of a continuos surface are limited to ± 1 pel. Therefore, in a second step neighboring regions with a disparity difference of ± 1 are merged. The remaining corona effect of block–matching is compensated during segmentation by adapting segmented region boundaries to neighboring luminance edges using an iterative dilation and skeletonization technique. Disparity values inside the corona are not considered during interpolation. Therefore the corona effect is avoided in the resulting depth map.

Beside its usage in DISTIMA, the presented algorithm has successfully been applied to modelling of 3D natural objects from multiple views in the RACE–MONA LISA project [2] and modelling of buildings from stereoscopic image sequences [10].

6 References

[1] R. Koch, "Model–Based 3D Scene Analysis from Stereoscopic Image Sequences", ISPRS '92, Vol. 29, Part B5, Washington, October 1992, pp. 427 – 437.

[2] Niem, W., Buschmann, R., "Automatic Modelling of 3D Natural Objects from Multiple Views", European Workshop on Combined real and synthetic image

processing for broadcast and video productions, 23–24. 11. 1994, Hamburg, Germany.

[3] L. Falkenhagen, A. Kopernik, M. Strintzis, ”Disparity Estimation based on 3D Arbitrarily Shaped Regions”, RACE Project Deliverable, R2045/UH/DS/P/023/b1

[4] A. Koschan, ”Eine Methodenbank zur Evaluierung von Stereo–Vision–Verfahren”, Ph. D Thesis, Technische Universität Berlin, Berlin, Germany, 1991.

[5] M. Bierling, ”Hierarchische Displacementschätzung zur Bewegungskompensation in digitalen Fernsehbildsequenzen”, Ph. D Thesis, Universität Hannover, Hannover, Germany, 1991.

[6] B. Choquet, A. Poussier, ”Selection of short existing test sequences”, RACE Project Deliverable, R2045/CCETT/WP3.1/DS/T/004/01

[7] Y. Yakimovski, R. Cunningham, ”A System for Extracting 3D Measurements from a Stereo Pair of TV Cameras”, CGVIP, Vol. 7, 1978, pp. 195 – 210.

[8] Cox, I., Hingorani, S., Maggs, B., Rao, S., ”Stereo without Regularisation”, NEC Research Institute, Princeton, NJ, USA, Oct. 1992.

[9] D. Terzopolus, ”The computation of visible surface representation”, IEEE Trans. Pattern Analysis and Machine Intelligence, Vol. 10, pp.417–438, USA, 1988.

[10] Koch, R., ”3–D Scene Modelling from Stereoscopic Image Sequences”, European Workshop on Combined real and synthetic image processing for broadcast and video productions, 23–24. 11. 1994, Hamburg, Germany.